

Contribution of Large Marine Aerosols in Phytoplankton Dispersal

Gregory Sinnett,* Luc Lenain, Emna Braham, Nabihah A. Chaudhry, and Julie Dinasquet*



Cite This: <https://doi.org/10.1021/acs.est.4c14473>



Read Online

ACCESS |

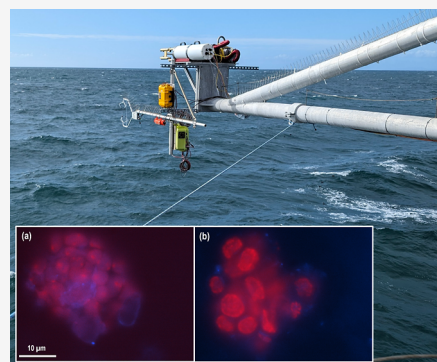
Metrics & More

Article Recommendations

Supporting Information

ABSTRACT: Sea-spray aerosol (SSA) plays a crucial role in climate processes by influencing radiative forcing, cloud formation, and precipitation. While SSA particles with diameters between 0.1 and 10 μm are commonly studied, larger aerosols ($>20 \mu\text{m}$) have been observed over terrestrial and oceanic regions but are generally overlooked. Large bioaerosols can be formed by pollen, fungal spores, and cell debris. However, the abundance, dynamics, and composition of large marine aerosols remain poorly understood. This study observed wave and atmospheric conditions driving aerosol production, the resulting SSA abundance, and sizes (up to 90 μm), and collected collocated SSA samples for microscopy analysis during a two-month time period. SSA above 20 μm were frequently observed, containing a diverse range of intact phytoplankton cells, including small flagellates (2 μm), to diatoms, and colonial cells (above 40 μm). The abundance of small flagellates suggests that sea-to-air transfer may be an important, yet overlooked, dispersal mechanism for these groups. To the best of our knowledge, this is the first evidence of direct airborne observation (rather than deposition) of large intact phytoplankton cells. These findings highlight the ubiquity of large marine aerosols and their capacity to carry intact phytoplankton cells.

KEYWORDS: aerosols, phytoplankton, transport, bioaerosols, large aerosols, sea-spray



INTRODUCTION

Sea-spray aerosol (SSA) represent one of the most abundant sources of natural aerosol particles in the atmosphere and play a crucial role on Earth's climate system, affecting cloud formation, precipitation patterns, and radiative forcing.^{1–3} SSA originate from the ocean surface through various mechanisms, including bubble bursting and wave breaking, which generate film and jet droplets, and the tearing of spume drops from wave crests during high winds.^{4,5} The quantity, size, and composition of the emitted drops are determined by the physical and chemical properties of the ocean surface as well as wind stress.

Small marine aerosol droplets persist in the atmosphere for days to weeks, allowing them to disperse widely while significantly contributing to a range of important climate processes.⁵ Recent efforts to characterize small aerosol production and distribution, e.g., Moore et al. (2022),⁶ have been motivated in part due to their significance to the global short- and long-wave radiation budget,⁷ sea salt flux,⁸ and potential as cloud nucleation sites.⁹ Marine aerosols can play a significant role in transporting microorganisms and organic matter into the atmosphere. These aerosols carry a diverse array of bacteria, viruses, and even phytoplankton especially cyanobacteria and chlorophyta but also larger taxa like diatoms and dinoflagellates, e.g., Wiśniewska et al. 2022¹⁰ and reviewed in Alsante et al. 2021,¹¹ Tesson et al. 2016,¹² and references therein. Airborne microorganism transport and dispersal has potential effects on ecology, climate, and public health.^{13–15}

Conversely, large aerosols ($>20 \mu\text{m}$) persist in the still atmosphere for seconds to minutes before gravitationally settling, yet in the real (turbulent) atmosphere, large aerosols have been observed above the ocean up to the top of the marine atmospheric boundary layer ($\approx 400 \text{ m}$) in small concentrations.^{16–18} LES modeling studies have supported these observations by demonstrating eddies are capable of transporting large aerosols hundreds of meters above the sea surface.¹⁹ The contribution large aerosols have to the ocean-atmosphere heat, salt, and momentum flux is potentially important in storm systems,^{19,20} though their overall climate effect and their potential to transport important molecules or particles is poorly understood given our limited understanding of their abundance and distribution in the atmosphere. Under high wind and wave conditions, large aerosols can be particularly important for cloud formation, as they can act as cloud condensation nuclei, potentially influencing precipitation and impacting the radiative properties of clouds. Detection limits and methodological choices have limited the number of observational studies relating large aerosol production and transport to ocean and atmospheric conditions, though numerical simulations indicate wave age, type and steepness

Received: December 24, 2024

Revised: February 20, 2025

Accepted: March 14, 2025

affect large aerosol injection to the atmosphere²¹ and hint at the importance that waves, coupled with wind, have on generating large aerosols.

While the aerosolization of marine bacteria has been relatively well-studied, e.g., Fahlgren et al.,²² Lang-Yona et al.,²³ Dinasquet et al.,²⁴ airborne phytoplankton transport has received less attention, potentially due to their lower abundance in the atmosphere ($0\text{--}10^4$ cells per cubic meter of air), the challenges associated with aerosolizing larger cells, and the focus on studying smaller aerosols.^{12,25} Hence, global airborne phytoplankton dispersal and subsequent effects on climate and ecosystems are unknown and require further research^{12,26} in support of integrated ecosystem, animal, and human health efforts (e.g., WHO “One Health”²⁷).

Airborne bacteria’s direct influence on atmospheric processes and cloud formation, in particular, through their ice nucleating capacities, is relatively well studied.²⁸ Despite evidence of phytoplankton, ranging from small cyanobacteria to large diatoms, contributing to ice nucleating particle formation, the specific processes associated with exudate emission or aerosolization of cell and cell fragments with ice nucleating properties still remain poorly understood.^{29–33} Furthermore, airborne phytoplankton transport has implications for public health.^{25,34} Some phytoplankton toxins can cause respiratory and skin irritation, and other cellular components may trigger allergic reactions.³⁵ Understanding phytoplankton aerosolization is therefore crucial for developing predictive models to protect public health.

Existing research on airborne phytoplankton dispersal often relies on observations of passive cell deposition and subsequent identification from selective cell culturability methods,^{10,12,26,36} which may not accurately reflect natural conditions. Direct evidence of airborne phytoplankton cells is still lacking, hindering our understanding of their dispersal patterns and potential impacts and motivating this work. In particular, the potential for the overlooked large marine aerosols to transport large phytoplankton cells has not been investigated. This study addresses this gap by presenting observations from a 2 month field experiment that provides direct evidence of phytoplankton transport through marine aerosols. We characterize large marine aerosols (up to $90\ \mu\text{m}$) in the coastal atmosphere and analyze the heterogeneity of phytoplankton cells they carry.

MATERIAL AND METHODS

In Situ Data Collection. Aerosol data, along with coincident atmospheric and ocean surface conditions, were collected at the end of the Ellen Browning Scripps Memorial Pier at the Scripps Institution of Oceanography (hereafter SIO Pier) during 31 days between June 27, 2024 and August 26, 2024. The SIO pier is a 330 m long structure extending into the Pacific Ocean approximately 200 m beyond the surf zone at mean tide. The SIO Pier deck is roughly 10 m above the ocean surface, and a maneuverable boom arm extends approximately 6 m from the end to position instruments over the water surface and away from the pier deck (Figure 1).

A Droplet Measurement Technologies FM-120 optical spectrometer (FM-120), a Droplet Measurement Technologies cloud imaging probe (CIP) optical spectrometer, and a Bertin Technologies Coriolis μ air sampler (Coriolis) were attached to the SIO Pier boom arm and deployed 10 m above mean sea level. Together, they sampled aerosol particle size distributions and collected aerosol samples for biological composition analysis (inset, Figure 1). The retractable boom arm allowed



Figure 1. Instrument deployment configuration for this study at the SIO Pier end. Instruments were deployed side-by-side (inset) approximately 10 m above mean sea level on a retractable boom arm 6 m away from the SIO Pier structure.

for continuous powered operation and for cleaning, calibrating, and angular repositioning as needed. Additionally, atmospheric and surface wave conditions were concurrently observed at the SIO Pier by NOAA and the Coastal Data Information Program (CDIP) buoy 201, located 0.8 km from the end of the SIO pier at a 41 m water depth.

Aerosol Measurements. The instrumented boom arm was deployed at an angle facing directly into the wind to maximize the aerosol collection efficiency and count accuracy. Data collection was limited to times when the mean wind speed was greater than $1\ \text{m s}^{-1}$, permitting the CIP to sample. Observations were made during both whitecapping and nonwhitecapping conditions. Wind angle was restricted to within $235^\circ < \theta < 325^\circ$, to avoid aerosol contamination from the surf zone and terrestrial sources. The wind angle restriction is supported by 3 h hindcast HYSPLIT particle trajectories initialized during sampling periods. These trajectories suggest that large aerosol particles (which are unlikely to stay suspended for longer than three h) most likely originated from offshore (Figure 2).

During times with optimal wind angles, the FM-120 continuously sampled the aerosol liquid water content (lwc) and particle size distributions between its 2 and $50\ \mu\text{m}$

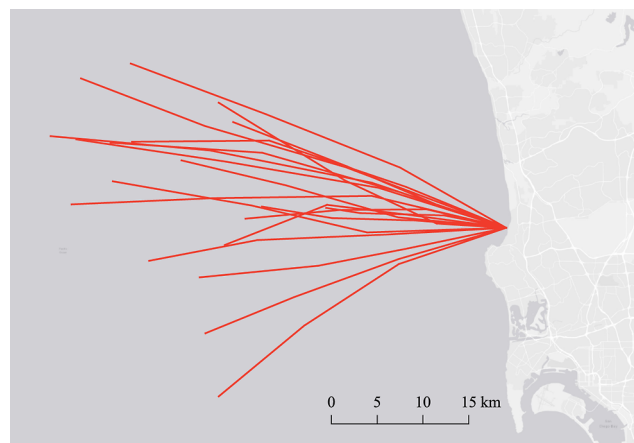


Figure 2. HYSPLIT 3 h hindcast trajectories for each sample day with origin at the SIO Pier experiment location.

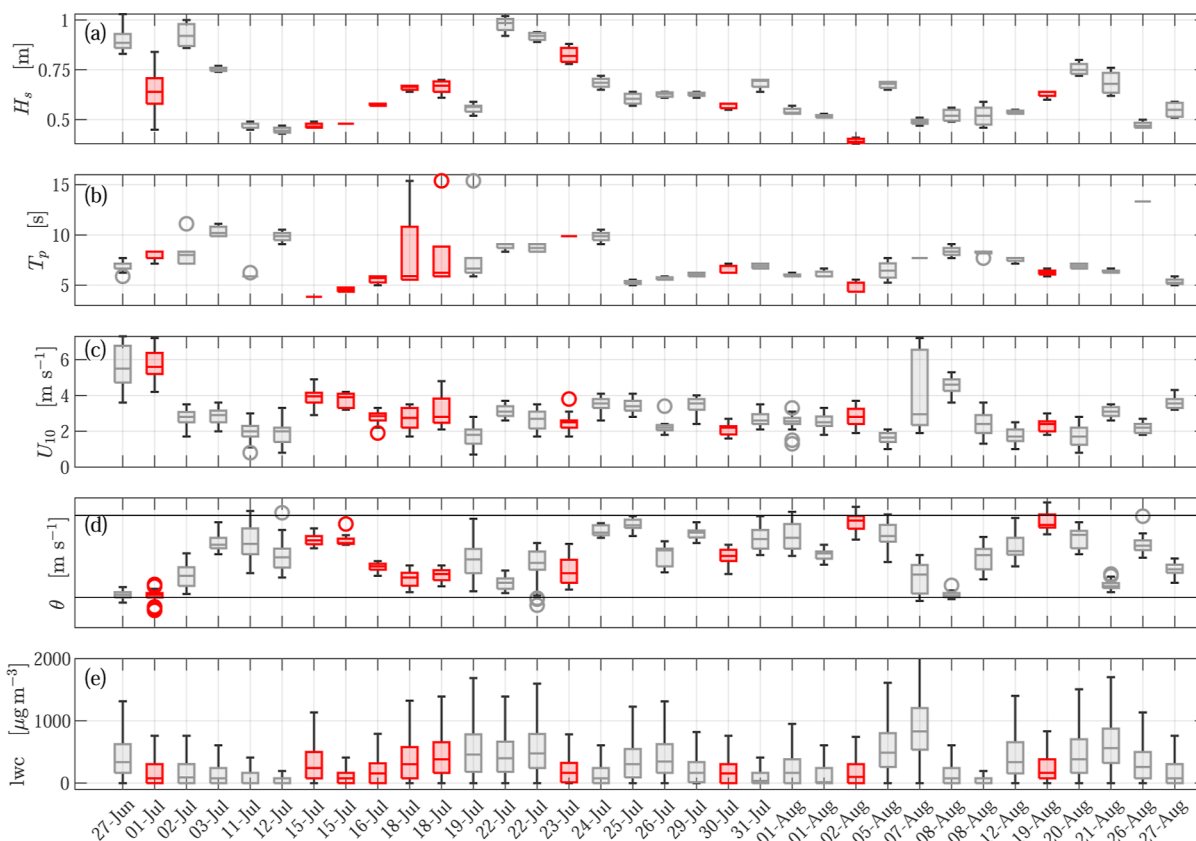


Figure 3. Background conditions during sampling periods spanning June 27, 2024 to August 27, 2024, including (a) significant wave height H_s , (b) wave peak period T_p , (c) wind speed 10 m above the mean ocean surface U_{10} , (d) wind direction θ with directional limits as black lines for reference, and (e) measured aerosol lwc observed during sample periods. Biologically interesting organisms were observed during most sample periods and are highlighted in red if they contain cell images presented in this paper. Note that some days had multiple sampling periods.

observational range, with $1 \mu\text{m}$ resolution for particle sizes between 2 and 14 and $2 \mu\text{m}$ resolution for particle sizes between 16 and $50 \mu\text{m}$. The FM-120 instrument draws air through a sampling chamber at a measured rate, allowing for a large air volume to be sampled in relatively calm conditions. The CIP optical spectrometer sampled particles of diameter between 15 and $930 \mu\text{m}$ with $15 \mu\text{m}$ resolution. The CIP instrument relies on air passing between a laser probe tip to sample aerosol distributions. Thus, the volume of sampled air depends on the wind speed. While sampling, both the FM-120 and CIP instruments recorded side-by-side counts of particles per resolved size bin at a 1 Hz sampling rate.

Following previous studies, e.g., Lenain and Melville (2017), an aerosol size distribution function was defined so that the total number of aerosol particles per unit volume of air is

$$N = \int_0^{\infty} n(D) dD \quad (1)$$

where $n(D) dD$ is the number of aerosol particles in the size class D to $D + dD$ in a unit volume of air. Both the FM-120 and CIP instruments measure particle counts in each resolved size bin $C(D)$, such that

$$n(D) = C(D)/V \quad (2)$$

where V is the sampled volume. The sampled FM-120 volume depends on the intake flow rate U_1 and sample area $A = 0.00287 \text{ cm}^2$ so that $V = U_1 \cdot A$. The CIP is an imaging probe and thus has a sampling volume dependent on the image depth of field (DOF) such that

$$V_i = \text{DOF}_i \cdot U_p \cdot t \cdot (63 - i) \cdot \zeta_i \quad (3)$$

where i is the particle bin number, ζ_i is the probe resolution of that bin, U_p is the air speed past the probe tips, t is the sample time, and DOF_i is the image DOF. Here, since the CIP has 62 imaging diodes, the sample volume width is size-bin-dependent, as a small particle can be counted if it crosses any of the 62 diodes, but a large particle (in bin 62, for example) can cross only the center of the array to be counted. Thus, the sample volume width is $(63 - i) \cdot \zeta_i$. Since the probe is fixed to the pier, $U_p = U_{10}$. The probe depth of field $\text{DOF}_i = F_i \cdot r_i / \lambda$ where the laser wavelength $\lambda = 658 \text{ nm}$, r_i is the mean radius of particles in bin i , and F_i is a factor that accounts for electronic response time and a 50% shadow threshold criterion.³⁷ Applying eqs 3 to 2, $n(D_i)$ can be estimated for any sampled period, where for convenience D_i is the maximum diameter in bin i .

Bioaerosol Measurements. The high air volume Coriolis air sampler (shown to effectively collect particles of diameters above $4 \mu\text{m}$)³⁸ fitted with the Long-term Monitoring Option (to avoid sample evaporation) collected coincident particle samples for microscopy analysis (inset, Figure 1). The Coriolis instrument continuously collected aerosols from air drawn at 100 L min^{-1} during the preselected 1–4 h sampling time periods. The air intake rate was optimized prior to the main sampling campaign after testing a range of intake rates from 100 to 300 L min^{-1} . Also, different collection media were tested, and a phytoplankton culture was used to determine cell resistance to centrifugal force and aggregate formation. An intake rate of 100 L min^{-1} was selected as it maximized the

collected sample volume, minimized damage to the integrity of the collected particles, and reduced the formation of aggregates caused by high turbulence within the collection vial. Samples were collected in phosphate-buffered saline buffer. Surface water samples were also collected during each sampling day at the SIO Pier. All aerosol and water sampling equipment was acid washed and rinsed between sampling periods. Additional seawater phytoplankton are continuously recorded through an in situ Imaging Flow Cytobot (IFCB 183, Southern California Coastal Ocean Observing System, SCCOOS program)³⁹ under the SIO Pier.

Samples were immediately processed in the laboratory after collection. A series of preliminary trials were conducted to optimize sample processing and microscopy image quality. Initial air sample aliquots were filtered through a range of polycarbonate filters with pore sizes from 0.2 to 10 μm to determine the optimal pore size for observing the desired size range of phytoplankton. Based on these trials, 3 μm pore-size filters were selected, as they provided the clearest images and captured the phytoplankton size range of greatest interest for this study. In addition to filtration, the use of Utermöhl chambers was tested for settling Lugol-fixed samples, with the aim of identifying larger phytoplankton cells that might be missed by filtration. However, this method did not yield superior results compared to the 3 μm filtration.

The Coriolis sampled between 6000 and 24,000 L of air depending on the sample duration, collecting aerosolized particles in a concentrated 15 mL vial. A 4 mL volume drawn from this 15 mL concentrated sample was found to be optimum for microscopy processing (after testing a range between 1 and the entire 15 mL). This volume provided a balance between sufficient cell density for representative analysis and image quality yet minimized obscuration from overlapping cells and debris.

For routine sample processing, 4 mL aliquots were fixed with 2% formaldehyde (0.2 μm filtered) and fixed for 10 min at 4 °C. Samples were then filtered through a 3 μm pore size polycarbonate filter (Millipore), stained with DAPI (4',6-diamidino-2-phenylindole) mixed with antifade (Vector Laboratories), and mounted on microscope slides. Samples were imaged by epifluorescence microscopy using a Nikon Eclipse Ti microscope. Cells showing red FITC autofluorescence (as a proxy for chlorophyll) were measured along their longest dimension. Only cells with both Chlorophyll autofluorescence and DAPI epifluorescence (blue, as a proxy for DNA) were considered in this study to avoid potential counts of terrestrial bioaerosols such as pollen, spores, and other fluorescence particles. Surface water samples collected at the end of the Pier were analyzed using the same procedure with 2 mL aliquots.

RESULTS AND DISCUSSION

Environmental Conditions. In total, 71 h of data were collected during 34 sampling periods spanning two months under a variety of wind, wave, and biological background conditions. The CDIP wave buoy recorded average wave height H_s and peak period T_p at 30 min intervals (Figure 3a,b). Wave heights ranged over 0.4 m < H_s < 1.1 m (Figure 3a) with periods 4 s < T_p < 16 s, occasionally creating whitecaps (Figure 3b). However, most sampled conditions were predominantly whitecap free.

Background atmospheric conditions, including wind speed U_{10} and wind direction θ , were observed at six min intervals by

the SIO pier by NOAA met station 9410230. U_{10} ranged from 1 to 8 m s⁻¹ (Figure 3c). Wind was observed from all directions during the two month observational period; however, aerosol observations were made only when wind was from the ocean, and subsequent data processing restricted data to periods where average wind angle was within the range 235° < θ < 325° to prevent contamination from the surf zone or land (Figure 3d).

Aerosol Observations. During the sample periods, I_{wc} varied from below detection limits to 23, 254 $\mu\text{g L}^{-1}$ (Figure 3e). Aerosols were observed during the experimental period varying in diameter between the instrument resolution thresholds of up to 90 μm . Number concentrations $n(D)$ for aerosols with diameters in the range 2 μm < D < 20 μm rolled off with a D^{-5} power law dependency as previously observed under similar conditions¹⁶ and varied over an order of magnitude (colored, Figure 4). These results are in good

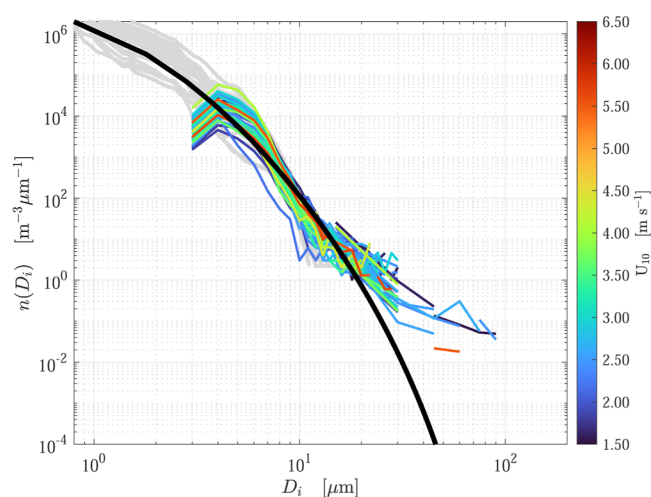


Figure 4. Aerosol number distribution as a function of binned diameter D_i for all sample periods. A common wind-dependent aerosol source parametrization (black line) is fit for reference using the average U_{10} over all observations. Aerosol observations from the 2023 EPCAPE experiment during the same June–August period (gray) are shown for additional context. U_{10} during each sampled period is indicated by color.

agreement with observations of aerosols from $D < 20 \mu\text{m}$ made a year earlier at roughly the same location during the Eastern Pacific Cloud Aerosol Precipitation Experiment (EPCAPE) experiment⁴⁰ (gray, Figure 4). Some slight wind dependency was observed (color gradient, Figure 4), though the relatively low average wind speeds did not constitute a large comparative signal, and we are thus unable to derive a functional wind speed dependence from these data. However, these results can be compared to an empirical log-normal mode source function parametrization

$$n(r_{80}) = n_0 \exp \left\{ -\frac{1}{2} \left[\frac{\ln(r_{80}/r'_{80})}{\ln \sigma} \right]^2 \right\} \quad (4)$$

where r_{80} is the equilibrium aerosol radius at an equivalent 80% relative humidity, n_0 is the maximum amplitude (a function of U_{10}), and σ is the size geometric standard deviation.^{7,41} In comparing the wind-dependent source function parametrization to aerosol number distribution observations, we assume that aerosols are vertically transported with a modification due

to gravity settling following Fairall et al. 2009⁴² so that at a given elevation z above the sea surface

$$n(D, z) = n(r_{30}) \left(\frac{z}{h_0} \right)^{(-v_d Sc_t) / (\kappa u_d f_s)} \quad (5)$$

where h_0 is the upper limit of the source region here taken to be the wave height, Sc_t is the droplet turbulent Schmidt number, and f_s is a slip factor. The settling velocity v_d is dependent on particle size d , the seawater density ρ_w , and air viscosity μ ,¹⁶ such that

$$v_d = \frac{\rho_w D^2 g}{18\mu} C_c(D) \quad (6)$$

where $C_c(D)$ is the Cunningham factor, a function of particle diameter, accounting for reduced surface slippage in small ($<10 \mu\text{m}$) particles.

This wind-dependent source function parametrization (4) for a logarithmic wind profile with $n_0 = 9 \times 10^{-4} U_{10}^2$ and $\sigma = 2.1$ is compared to aerosol number distribution observations (Figure 4). We find general consistency between the wind-dependent parametrization and the observed aerosol distribution for sizes smaller than $20 \mu\text{m}$. Sensitivity to wind speed (and thus the aerosol production fetch) is also consistent, as the parametrization predicts $n(D)$ over the same range as the observations.

Large aerosols ($20 \mu\text{m} < D$) were commonly observed, with only three observational periods (out of 34) containing no aerosols larger than $20 \mu\text{m}$. Large aerosols were also observed during all wind conditions (color, Figure 4) indicating that strong wind is not necessarily required to generate these particles. Further, the wind-dependent source parametrization (black, Figure 4) consistently underpredicts the observed large aerosol $n(D)$ at $z = 10 \text{ m}$. Both these results indicate that large aerosols may be more ubiquitous under average ocean conditions than current wind-dependent parametrized estimates, such as eq 5, predict.

The vertical settling velocity v_d varied between 1.25 and 25.3 cm s^{-1} for large aerosols observed in this study ($20 \mu\text{m} < D < 90 \mu\text{m}$). Making the conservative assumption that there is negligible average vertical turbulent flux (neglecting areas of strong updrafts or downdrafts) and applying the average observed horizontal wind speed in this study, $U_{10} = 2.4 \text{ m s}^{-1}$, these large aerosols would have taken between 40 and 800 s to settle back to the ocean surface and traveled between 100 m and 2 km while settling from the observed 10 m height. The true horizontal range for some of these large aerosols is presumably larger since $z = 10 \text{ m}$ is not the ceiling but rather only the observational height of this study, and the horizontal distance required for an aerosol particle to first obtain an elevation of 10 m above the sea surface is not accounted for in this estimate. Thus, aeolian transport of aerosols larger than $20 \mu\text{m}$ may regularly occur at regional scales of several kilometers, motivating future work to characterize large aerosol production, entrainment, and transport.

Aerosol Biological Composition. Phytoplankton cells ranging in size from 2 to $40 \mu\text{m}$ were observed in all aerosol samples and encompassed a large taxonomic range. For example, direct (not cultured) observations of picoplankton (Figure S1) to larger colonial *Phaeocystis* (Figure 5) were observed. Previous studies have identified airborne phytoplankton (both from marine and freshwater origins), ranging in

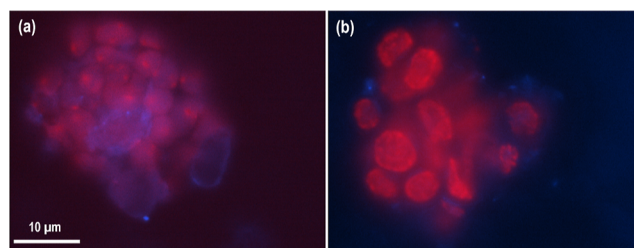


Figure 5. Epifluorescence microscope images of putative colonial *Phaeocystis* sp. observed in air samples collected on 07/01/24 (a) and 08/02/24 (b). Red indicates autofluorescence of photosynthetic pigments, and blue indicates DAPI staining of DNA. Note $10 \mu\text{m}$ scale in (a).

size from 1 to $500 \mu\text{m}$, including diatoms and dinoflagellates, e.g., Tesson et al.¹² and Wiśniewska et al.¹⁰ These studies relied on the selective cultivation of phytoplankton from passively deposited aerosols. Our research builds upon these works by directly observing intact airborne cells within marine aerosols.

Phytoplankton taxa observed in aerosol and water samples from the SIO Pier end overlapped. Comparison with in situ IFCB data at the SIO Pier from the SCCOOS network³⁹ further confirms the concurrent presence of the taxa observed both in the air and in the local surface seawater (Figures S3–S5). This result is expected, especially given the estimated several kilometers generation region for large sea spray aerosols and highlighted by possible hindcast trajectories (Figure 2). However, water samples collected at the SIO pier may not perfectly represent the offshore source water for aerosols generated further from the coast. While the seawater imaging confirm the presence of many of the observed aerosolized phytoplankton taxa in the local seawater, the heterogeneity observed with IFCB compared to air samples suggests a selective aerosolization process where all phytoplankton cells are not equally transferred into the aerosols. Selectivity of aerosolization processes have been observed for bacteria and viruses.^{22,24,43} This potential selective transfer is likely associated with cell morphology, size, and biomass but requires further study.

Small picoplankton and nanoflagellates (Figures 6 and S1), likely associated with Cryptophytes or Prymniophytes, were observed on a regular basis. The high occurrence of nanoplankton in our marine aerosol direct observations is remarkable, also consistent with sea surface microlayer (SML) observations of nanoplankton enrichment.⁴⁴ The SML has been shown to be a precursor to bacteria and virus aerosolization and to affect selective transfer of cells.^{24,43,45} This selective transfer process is likely similar for small phytoplankton cells like nanoflagellates. The frequent direct nanoplankton observations in this study suggest that sea-to-air transfer could influence nanoflagellate dispersal and thus their biogeography and ecosystem impact. Nanoflagellates have also been shown to have significant impact on atmospheric chemistry and aerosol production^{46,47} but the processes associated with this phenomenon are unknown, highlighting the need for further investigation of nanoplankton direct and indirect influence on atmospheric chemistry and climate.

Large cells associated with known bloom-forming taxa such as *Phaeocystis* sp. and diatoms were also occasionally observed (Figures 5 and 7). Diatom taxa such as *Chaetoceros* sp., *Coscinodiscus* sp., and *Nitzschia* sp. have been reported from

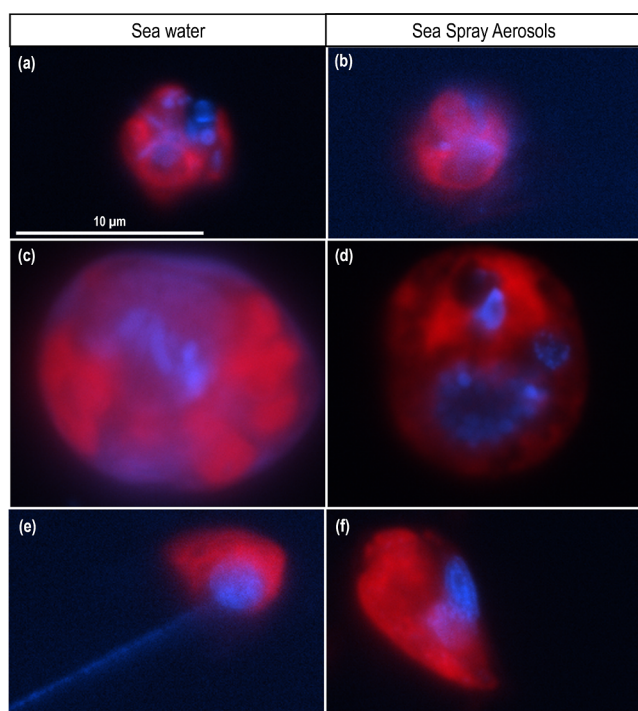


Figure 6. Epifluorescence microscope images of nanophytoplankton cells observed in the seawater (left) and sea spray aerosol air samples (right). (a–f) Collected on 08/07/24, 07/18/24, 07/23/24, 07/16/24, 07/16/24, and 07/18/24 respectively. Red indicates autofluorescence of photosynthetic pigments, and blue indicates DAPI staining of DNA. Note 10 μm scale in (a).

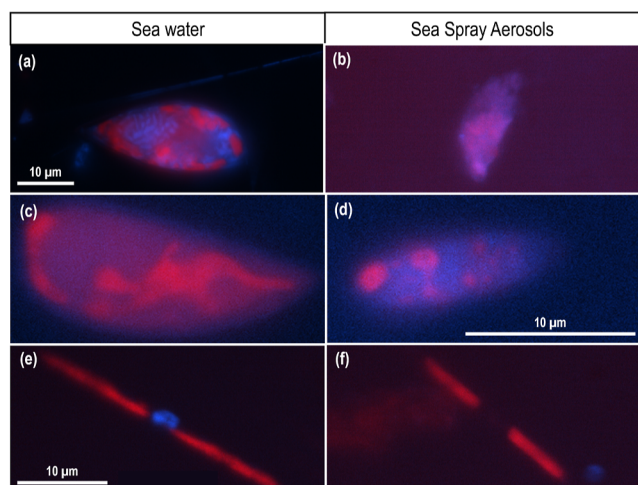


Figure 7. Epifluorescence microscope images of putative diatoms observed in seawater (a,c,e) and air (b,d,f) samples collected around 07/23/24 and 07/29/24. Red indicates autofluorescence of photosynthetic pigments, and blue indicates DAPI staining of DNA. Note 10 μm scale in (a) for (a,b), in (d) for (c,d) and in (e) for (e,f).

deposition studies.¹² As demonstrated in this study, the large intact aerosolized cells observed here 10 m above the water level have the potential to be transported several kilometers. Long range transport of phytoplankton could have significant ecological implications for harmful algal bloom (HAB) geographic expansion. Moreover, some HABs produce toxins, making their dispersal dynamics and potential impacts on human respiratory health and skin allergies important. Airborne toxins may be particle-associated;⁴⁸ the presence of

intact toxic cells or cell fragments in aerosols⁴⁹ suggests the possibility of inhalation exposure and dermatitis, warranting further health impact studies. Moreover, the presence of intact *Phaeocystis* colonies and diatoms, known to produce volatile organic compounds in surface waters that can influence atmospheric chemistry and particle formation,^{50,51} raises the question on their potential activity and role on atmospheric processes while airborne. Foam production during *Phaeocystis* blooms⁵² could be a mechanism for surface enrichment and sea-air transfer of cells.

Notably, aggregates (Figure S2) were observed in aerosols but were not apparent in the seawater samples. This suggests that aggregation likely occurred within individual evaporating droplets as they concentrated cells, debris, and exopolymer particles, or during centrifugal aggregation during collection.⁵³ Conversely, cell fragmentation could be due to aerosol collection methods or the product of sea-to-air transfer. SML and aerosols are known to be enriched in transparent exopolymers^{54–56} which could influence the aggregation of cell debris during aerosolization. Full phytoplankton cells or cell debris aggregates may have a significant impact on climate and cloud formation through their chemical properties. These direct observations of a wide range of aerosolized cell taxa and sizes motivate further investigation to better constrain the direct and indirect phytoplankton aerosol dynamics and its effect on climate and ecology. Future studies could also focus on emission mechanisms and cell adaptation to hostile atmospheric conditions such as UV, desiccation, and temperatures during dispersal.

Contextual Significance. Despite relatively mild wind and wave conditions over the 2 month sampling period, aerosols with diameters $D > 20 \mu\text{m}$ were consistently observed at higher concentrations than those predicted by commonly applied wind speed-dependent parametrizations. These results indicate that large aerosols are more ubiquitous above the ocean surface than commonly assumed, supporting previous observations of large aerosols at elevations up to 400 m.^{16–18} We find commonly applied log-normal mode wind-speed-dependent parametrizations underpredict the number distribution of these large aerosols at 10 m elevation by several orders of magnitude, suggesting these models miss important physics related to large aerosol generation and transport. Consequently, large marine aerosols are frequently ignored by the biology and chemistry communities that often assume aerosols of such size gravitationally settle shortly after being generated. Rather, as laboratory studies and LES simulations have shown, large aerosol production may be higher than commonly thought^{42,57} and vertical transport may be enhanced by sea state and turbulent eddies.¹⁹ Our results support these findings and motivate a better understanding of large aerosol production, entrainment, and transport to help tune aerosol parametrizations accounting for large particle behavior.

Simultaneous collection of bioaerosols shows novel direct evidence of airborne intact marine phytoplankton cells representing a wide range of taxonomy, size, and morphology. Nano and Picoplankton were abundant in aerosol samples, confirming sea-to-air transfer is a potentially important biogeographic dispersal mechanism. Surprisingly larger intact cells such as *Phaeocystis* colonies and diatoms were observed in aerosols, further stressing the need to better understand the role of these airborne cells on atmospheric processes and ecosystem dynamics. Results from this study highlight the overlooked capacity large aerosols have as a biological

transport vector for a wide variety of cells, with implications for atmospheric chemistry and climate and both human and ecosystem dynamics. Future efforts to quantify biological diversity and dynamics within large aerosols will prove to be valuable. In particular, when wind or updrafts are stronger (such as within storms or hurricanes), we expect significantly higher production of larger aerosols that could transport larger phytoplankton cells over longer distances, with potential significant implications for human health.

■ ASSOCIATED CONTENT

SI Supporting Information

The Supporting Information is available free of charge at <https://pubs.acs.org/doi/10.1021/acs.est.4c14473>.

Epifluorescence microscope images comparing phytoplankton observed in air and water; epifluorescence microscope images of bacterial colonization observed in air samples; and IFCB images depicting in situ ocean observations while air sampling (PDF)

■ AUTHOR INFORMATION

Corresponding Authors

Gregory Sinnett – Scripps Institution of Oceanography and Marine Physical Laboratory, University of California, San Diego, California 92093, United States; orcid.org/0000-0002-5617-5366; Email: gsinnett@ucsd.edu

Julie Dinasquet – Scripps Institution of Oceanography and Marine Biology Research Division, University of California, San Diego, California 92093, United States; Email: jdinasquet@ucsd.edu

Authors

Luc Lenain – Scripps Institution of Oceanography and Marine Physical Laboratory, University of California, San Diego, California 92093, United States

Emna Braham – Scripps Institution of Oceanography and Marine Biology Research Division, University of California, San Diego, California 92093, United States

Nabihah A. Chaudhry – Scripps Institution of Oceanography and Marine Physical Laboratory, University of California, San Diego, California 92093, United States; orcid.org/0009-0003-3002-2075

Complete contact information is available at: <https://pubs.acs.org/doi/10.1021/acs.est.4c14473>

Notes

The authors declare no competing financial interest.

■ ACKNOWLEDGMENTS

The authors thank Nick Statom, Evan Harris, and Gabriel Gekas for valuable support testing and deploying the sampling instruments. The authors also thank Kayli Matsuyoshi for support with FM-120 data processing. Supporting Information was obtained from the Atmospheric Radiation Measurement (ARM) Program sponsored by the U.S. Department of Energy, Office of Science, Office of Biological and Environmental Research, Climate and Environmental Sciences Division; and from the California Imaging FlowCytobot (ICFB) Network (<https://sccoos.org/ifcb/>) through the publicly available portal (<https://ifcb.caloos.org/dashboard>). The IFCB plankton image data are the result of a large integrated observational effort. Four independent reviewers significantly improved the

quality of this manuscript. This work was supported by the Office of Naval Research under grants N00014-22-1-2256 and N00014-21-1-2825.

■ REFERENCES

- (1) Fitzgerald, J. W. Marine aerosols: A review. *Atmos. Environ., Part A* **1991**, *25*, 533–545.
- (2) Brooks, S. D.; Thornton, D. C. Marine Aerosols and Clouds. *Ann. Rev. Mar. Sci.* **2018**, *10*, 289–313.
- (3) Cochran, R. E.; Ryder, O. S.; Grassian, V. H.; Prather, K. A. Sea Spray Aerosol: The Chemical Link between the Oceans, Atmosphere, and Climate. *Acc. Chem. Res.* **2017**, *50*, 599–604.
- (4) O'Dowd, C. D.; de Leeuw, G. Marine aerosol production: a review of the current knowledge. *Phil. Trans. Math. Phys. Eng. Sci.* **2007**, *365*, 1753–1774.
- (5) Veron, F. Ocean Spray. *Annu. Rev. Fluid. Mech.* **2015**, *47*, 507–538.
- (6) Moore, K. A.; Alexander, S. P.; Humphries, R. S.; Jensen, J.; Protat, A.; Reeves, J. M.; Sanchez, K. J.; Kreidenweis, S. M.; DeMott, P. J. Estimation of Sea Spray Aerosol Surface Area Over the Southern Ocean Using Scattering Measurements. *J. Geophys. Res. Atmos.* **2022**, *127*, No. e2022JD037009.
- (7) Lewis, E. R.; Schwartz, S. E. *Sea Salt Aerosol Production Mechanisms, Methods, Measurements and Models*; American Geophysical Union: 2000 Florida Avenue, N.W. Washington, DC, 2004; Vol. 20009, p 17.
- (8) Textor, C.; Schulz, M.; Guibert, S.; Kinne, S.; Balkanski, Y.; Bauer, S.; Bernsten, T.; Berglen, T.; Boucher, O.; Chin, M.; Dentener, F.; Diehl, T.; Easter, R.; Feichter, H.; Fillmore, D.; Ghan, S.; Ginoux, P.; Gong, S.; Grini, A.; Hendricks, J.; Horowitz, L.; Huang, P.; Isaksen, I.; Iversen, I.; Kloster, S.; Koch, D.; Kirkevåg, A.; Kristjánsson, J. E.; Krol, M.; Lauer, A.; Lamarque, J. F.; Liu, X.; Montanaro, V.; Myhre, G.; Penner, J.; Pitari, G.; Reddy, S.; Seland, Ø.; Stier, P.; et al. Analysis and quantification of the diversities of aerosol life cycles within AeroCom. *Atmos. Chem. Phys.* **2006**, *6*, 1777–1813.
- (9) Andreae, M.; Rosenfeld, D. Aerosol–cloud–precipitation interactions. Part 1. The nature and sources of cloud-active aerosols. *Earth-Sci. Rev.* **2008**, *89*, 13–41.
- (10) Wiśniewska, K. A.; Śliwińska-Wilczewska, S.; Lewandowska, A. U. Airborne microalgal and cyanobacterial diversity and composition during rain events in the southern Baltic Sea region. *Sci. Rep.* **2022**, *12*, 2029.
- (11) Alsante, A. N.; Thornton, D. C. O.; Brooks, S. D. Ocean Aerobiology. *Front. Microbiol.* **2021**, *12*, 764178.
- (12) Tesson, S. V. M.; Skjøth, C. A.; Santl-Temkiv, T.; Löndahl, J. Airborne Microalgae: Insights, Opportunities, and Challenges. *Appl. Environ. Microbiol.* **2016**, *82*, 1978–1991.
- (13) Fröhlich-Nowoisky, J.; Kampf, C. J.; Weber, B.; Huffman, J. A.; Pöhlker, C.; Andreae, M. O.; Lang-Yona, N.; Burrows, S. M.; Gunthe, S. S.; Elbert, W.; Su, H.; Hoor, P.; Thines, E.; Hoffmann, T.; Després, V. R.; Pöschl, U. Bioaerosols in the Earth system: Climate, health, and ecosystem interactions. *Atmos. Res.* **2016**, *182*, 346–376.
- (14) Tastassa, A. C.; Sharaby, Y.; Lang-Yona, N. Aeromicrobiology: A global review of the cycling and relationships of bioaerosols with the atmosphere. *Sci. Total Environ.* **2024**, *912*, 168478.
- (15) Lang-Yona, N.; Flores, J. M.; Nir-Zadock, T. S.; Nussbaum, I.; Koren, I.; Vardi, A. Impact of airborne algicidal bacteria on marine phytoplankton blooms. *ISME J.* **2024**, *18*, wrac016.
- (16) Lenain, L.; Melville, W. K. Evidence of Sea-State Dependence of Aerosol Concentration in the Marine Atmospheric Boundary Layer. *J. Phys. Oceanogr.* **2017**, *47*, 69–84.
- (17) Reid, J. S.; Jonsson, H. H.; Smith, M. H.; Smirnov, A. Evolution of the vertical profile and flux of large sea-salt particles in a coastal zone. *J. Geophys. Res. Atmos.* **2001**, *106*, 12039–12053.
- (18) Reid, J. S.; Brooks, B.; Crahan, K. K.; Hegg, D. A.; Eck, T. F.; O'Neill, N.; de Leeuw, G.; Reid, E. A.; Anderson, K. D. Reconciliation of coarse mode sea-salt aerosol particle size measurements and

parameterizations at a subtropical ocean receptor site” regarding the use of aerodynamic particle sizers in marine environments. *J. Geophys. Res.* **2006**, *111*, D02202.

(19) Shpund, J.; Zhang, J. A.; Pinsky, M.; Khain, A. Microphysical Structure of the Marine Boundary Layer under Strong Wind and Spray Formation as Seen from Simulations Using a 2D Explicit Microphysical Model. Part II: The Role of Sea Spray. *J. Atmos. Sci.* **2012**, *69*, 3501–3514.

(20) Bianco, L.; Bao, J. W.; Fairall, C. W.; Michelson, S. A. Impact of Sea-Spray on the Atmospheric Surface Layer. *Boundary-Layer Meteorol.* **2011**, *140*, 361–381.

(21) Tang, S.; Yang, Z.; Liu, C.; Dong, Y.-H.; Shen, L. Numerical Study on the Generation and Transport of Spume Droplets in Wind over Breaking Waves. *Atmosphere* **2017**, *8*, 248.

(22) Fahlgren, C.; Gómez-Consarnau, L.; Zábori, J.; Lindh, M. V.; Krejci, R.; Mårtensson, E. M.; Nilsson, D.; Pinhassi, J. Seawater mesocosm experiments in the Arctic uncover differential transfer of marine bacteria to aerosols. *Environ. Microbiol. Rep.* **2015**, *7*, 460–470.

(23) Lang-Yona, N.; Flores, J. M.; Haviv, R.; Alberti, A.; Poulain, J.; Belser, C.; Trainic, M.; Gat, D.; Ruscheweyh, H.-J.; Wincker, P.; Sunagawa, S.; Rudich, Y.; Koren, I.; Vardi, A. Terrestrial and marine influence on atmospheric bacterial diversity over the north Atlantic and Pacific Oceans. *Commun. Earth Environ.* **2022**, *3*, 121.

(24) Dinasquet, J.; Zäncker, B.; Nicosia, A.; Bigeard, E.; Baudoux, A.-C.; Engel, A.; Guieu, C.; Obernosterer, I.; Sellegri, K. Marine bacterial enrichment in the sea surface microlayer, and surface taxa aerosolization potential in the Western Mediterranean Sea. *bioRxiv* **2023**, 2023.04.26.538450. DOI: [10.1101/2023.04.26.538450](https://doi.org/10.1101/2023.04.26.538450)

(25) Wiśniewska, K.; Lewandowska, A.; Śliwińska-Wilczewska, S. The importance of cyanobacteria and microalgae present in aerosols to human health and the environment – Review study. *Environ. Int.* **2019**, *131*, 104964.

(26) Sahu, N.; Tangutur, A. D. Airborne algae: overview of the current status and its implications on the environment. *Aerobiologia* **2015**, *31*, 89–97.

(27) World Health Organization. One Health Initiative, 2024. <https://www.who.int/teams/one-health-initiative> (accessed February 4, 2025).

(28) Šantl-Temkiv, T.; Amato, P.; Casamayor, E. O.; Lee, P. K. H.; Pointing, S. B. Microbial ecology of the atmosphere. *FEMS Microbiol. Rev.* **2022**, *46*, fuac009.

(29) Knopf, D. A.; Alpert, P. A.; Wang, B.; Aller, J. Y. Stimulation of ice nucleation by marine diatoms. *Nat. Geosci.* **2011**, *4*, 88–90.

(30) Wolf, M. J.; Coe, A.; Dove, L. A.; Zawadowicz, M. A.; Dooley, K.; Biller, S. J.; Zhang, Y.; Chisholm, S. W.; Cziczó, D. J. Investigating the Heterogeneous Ice Nucleation of Sea Spray Aerosols Using *Prochlorococcus* as a Model Source of Marine Organic Matter. *Environ. Sci. Technol.* **2019**, *53*, 1139–1149.

(31) Creamean, J. M.; Cross, J. N.; Pickart, R.; McRaven, L.; Lin, P.; Pacini, A.; Hanlon, R.; Schmale, D. G.; Cenicerros, J.; Aydeell, T.; Colombi, N.; Bolger, E.; DeMott, P. J. Ice Nucleating Particles Carried From Below a Phytoplankton Bloom to the Arctic Atmosphere. *Geophys. Res. Lett.* **2019**, *46*, 8572–8581.

(32) Thornton, D. C. O.; Brooks, S. D.; Wilbourn, E. K.; Mirrielees, J.; Alsante, A. N.; Gold-Bouchot, G.; Whitesell, A.; McFadden, K. Production of ice-nucleating particles (INPs) by fast-growing phytoplankton. *Atmos. Chem. Phys.* **2023**, *23*, 12707–12729.

(33) Eickhoff, L.; Bayer-Giraldi, M.; Reicher, N.; Rudich, Y.; Koop, T. Ice nucleating properties of the sea ice diatom *Fragilariopsis cylindrus* and its exudates. *Biogeosciences* **2023**, *20*, 1–14.

(34) Dey, S.; Wiśniewska, K. A.; Śliwińska-Wilczewska, S.; Mitra, A.; Błaszczak, A.; Chatterjee, B.; Dey, S.; Lewandowska, A. U. Deposition of airborne cyanobacteria and microalgae in the human respiratory tract (Baltic Sea coastal zone, Poland). *Mar. Pollut. Bull.* **2024**, *207*, 116883.

(35) Lim, C. C.; Yoon, J.; Reynolds, K.; Gerald, L. B.; Ault, A. P.; Heo, S.; Bell, M. L. Harmful algal bloom aerosols and human health. *EBioMedicine* **2023**, *93*, 104604.

(36) Wiśniewska, K.; Śliwińska-Wilczewska, S.; Lewandowska, A. The first characterization of airborne cyanobacteria and microalgae in the Adriatic Sea region. *PLoS One* **2020**, *15*, No. e0238808.

(37) Baumgardner, D.; Korolev, A. Airspeed Corrections for Optical Array Probe Sample Volumes. *J. Atmos. Ocean. Technol.* **1997**, *14*, 1224–1229.

(38) Carvalho, E.; Sindt, C.; Verdier, A.; Galan, C.; O'Donoghue, L.; Parks, S.; Thibaudon, M.; Thibaudon, M. Performance of the Coriolis air sampler, a high-volume aerosol-collection system for quantification of airborne spores and pollen grains. *Aerobiologia* **2008**, *24*, 191–201.

(39) Barton, A. D.; Bowman, J. S.; Kenitz, K. M. Scripps Pier (Instrument ID: IFCB183). In *California Imaging FloCytobot Network (CA IFCB Network)*; UC San Diego Library Digital Collections, 2025.

(40) Atmospheric Radiation Measurement (ARM) user facility. Aerodynamic Particle Sizer (AOSAPS), 2023–02–15 to 2024–02–14, ARM Mobile Facility (EPC) La Jolla, CA; AMF1 (main site for EPCAPE on Scripps Pier) (M1). Compiled by A. Singh, D. Oliveira, A. Koontz, A. Sedlacek and C. Kuang. ARM Data Center. Data set–02–04, 2023. <https://urldefense.com/v3/> (accessed Feb 04, 2025).

(41) Jones, K. F.; Andreas, E. L. Sea spray concentrations and the icing of fixed offshore structures. *Q. J. R. Meteorol. Soc.* **2012**, *138*, 131–144.

(42) Fairall, C. W.; Banner, M. L.; Peirson, W. L.; Asher, W.; Morison, R. P. Investigation of the physical scaling of sea spray spume droplet production. *J. Geophys. Res. Oceans* **2009**, *114*, DOI: DOI: .

(43) Michaud, J. M.; Thompson, L. R.; Kaul, D.; Espinoza, J. L.; Richter, R. A.; Xu, Z. Z.; Lee, C.; Pham, K. M.; Beall, C. M.; Malfatti, F.; Azam, F.; Knight, R.; Burkart, M. D.; Dupont, C. L.; Prather, K. A. Taxon-specific aerosolization of bacteria and viruses in an experimental ocean-atmosphere mesocosm. *Nat. Commun.* **2018**, *9*, 2017.

(44) Joux, F.; Agogue, H.; Obernosterer, I.; Dupuy, C.; Reinthaler, T.; Herndl, G. J.; Lebaron, P. Microbial community structure in the sea surface microlayer at two contrasting coastal sites in the northwestern Mediterranean Sea. *Aquat. Microb. Ecol.* **2006**, *42*, 91–104.

(45) Aller, J. Y.; Kuznetsova, M. R.; Jahns, C. J.; Kemp, P. F. The sea surface microlayer as a source of viral and bacterial enrichment in marine aerosols. *J. Aerosol Sci.* **2005**, *36*, 801–812.

(46) Sellegri, K.; Nicosia, A.; Freney, E.; Uitz, J.; Thyssen, M.; Grégori, G.; Engel, A.; Zäncker, B.; Haëntjens, N.; Mas, S.; Picard, D.; Saint-Macary, A.; Peltola, M.; Rose, C.; Trueblood, J.; Lefevre, D.; D'Anna, B.; Desboeufs, K.; Meskhidze, N.; Guieu, C.; Law, C. S. Surface ocean microbiota determine cloud precursors. *Sci. Rep.* **2021**, *11*, 281.

(47) Dall'Osto, M.; Vaqué, D.; Sotomayor-García, A.; Cabrera-Brufau, M.; Estrada, M.; Buchaca, T.; Soler, M.; Nunes, S.; Zeppenfeld, S.; van Pinxteren, M.; Herrmann, H.; Wex, H.; Rinaldi, M.; Paglione, M.; Beddows, D. C. S.; Harrison, R. M.; Berdalet, E. Sea Ice Microbiota in the Antarctic Peninsula Modulates Cloud-Relevant Sea Spray Aerosol Production. *Front. Mar. Sci.* **2022**, *9*, 827061.

(48) Ternon, E.; Dinasquet, J.; Cancelada, L.; Rico, B.; Moore, A.; Trytten, E.; Prather, K. A.; Gerwick, W. H.; Lemée, R. Sea-Air Transfer of *Ostreopsis* Phycotoxins Is Driven by the Chemical Diversity of the Particulate Fraction in the Surface Microlayer. *Environ. Sci. Technol.* **2024**, *58*, 18969–18979.

(49) Casabianca, S.; Casabianca, A.; Riobó, P.; Franco, J.; Vila, M.; Penna, A. Quantification of the Toxic Dinoflagellate *Ostreopsis* spp. by qPCR Assay in Marine Aerosol. *Environ. Sci. Technol.* **2013**, *47*, 3788–3795.

(50) Liss, P.; Malin, G.; Turner, S.; Holligan, P. Dimethyl sulphide and Phaeocystis: A review. *J. Mar. Syst.* **1994**, *5*, 41–53.

(51) Dani, K. S.; Benavides, A. M. S.; Michelozzi, M.; Peluso, G.; Torzillo, G.; Loreto, F. Relationship between isoprene emission and photosynthesis in diatoms, and its implications for global marine isoprene estimates. *Mar. Chem.* **2017**, *189*, 17–24.

(52) Lancelot, C. The mucilage phenomenon in the continental coastal waters of the North Sea. *Sci. Total Environ.* **1995**, *165*, 83–102.

(53) van Pinxteren, M.; Robinson, T.-B.; Zeppenfeld, S.; Gong, X.; Bahlmann, E.; Fomba, K. W.; Triesch, N.; Stratmann, F.; Wurl, O.; Engel, A.; Wex, H.; Herrmann, H. High number concentrations of transparent exopolymer particles in ambient aerosol particles and cloud water – a case study at the tropical Atlantic Ocean. *Atmos. Chem. Phys.* **2022**, *22*, 5725–5742.

(54) Wurl, O.; Holmes, M. The gelatinous nature of the sea-surface microlayer. *Mar. Chem.* **2008**, *110*, 89–97.

(55) Robinson, T.-B.; Giebel, H.-A.; Wurl, O. Riding the Plumes: Characterizing Bubble Scavenging Conditions for the Enrichment of the Sea-Surface Microlayer by Transparent Exopolymer Particles. *Atmosphere* **2019**, *10*, 454.

(56) Aller, J. Y.; Radway, J. C.; Kilhau, W. P.; Bothe, D. W.; Wilson, T. W.; Vaillancourt, R. D.; Quinn, P. K.; Coffman, D. J.; Murray, B. J.; Knopf, D. A. Size-resolved characterization of the polysaccharidic and proteinaceous components of sea spray aerosol. *Atmos. Environ.* **2017**, *154*, 331–347.

(57) Veron, F.; Hopkins, C.; Harrison, E. L.; Mueller, J. A. Sea spray spume droplet production in high wind speeds. *Geophys. Res. Lett.* **2012**, *39*.